P1.22 INTERACTION OF A MOUNTAIN LEE WAVE WITH A BASIN COLD POOL

George S. Young, Brian J. Gaudet, Nelson L. Seaman, David R. Stauffer

Pennsylvania State University, University Park, Pennsylvania

1. INTRODUCTION

Mountain meteorology under stable stratification can exhibit a broad range of mesoscale phenomena (Beal et al. 2005). This modeling case study focuses on two of these: 1) drainage flow and the resultant valley-floor cold pool (Fast et al. 1996); and 2) cross-ridge flow and the resultant mountain lee waves (Scorer 1949). The two have usually been studied separately although they can partake in a two-way interaction as highlighted in this case study. In one direction, the drainage flow and cold pool affect the wind and stability profiles experienced by mountain lee waves, while in the other direction the waves affect the wind driven erosion (i.e. scouring) of the cold pool (Zhong et al. 2001). These interactions have been sparsely studied, in part due to the difficulties in taking comprehensive measurements of boundary layer evolution across a basin during mountain lee wave conditions.

Stability of the boundary layer underlying mountain lee waves can have a substantial impact on the structure and behavior of the waves (Grubišić et al. 2008; Doyle and Durran 2002). In particular, changes in the boundary layer stability due to surface heat fluxes can impact the intensity of both rotors and downslope windstorms (Jiang and Doyle 2008).

Likewise, the wind shear profile can have a profound impact on wave behavior (e.g. Scorer 1949, Durran and Klemp 1983). In particular, wave breaking occurs when the wind shear profile results in sufficient tilt of the phase planes for the isentropes to pass vertical at some point in the wave (Doyle et al. 2000). This can occur in conjunction with a critical level where the speed of mean flow perpendicular to the ridge goes to zero (Grubišić and Smolarkiewicz 1997).

The interaction between wave and mean wind profile can go in the opposite sense as well with wave breaking transferring momentum to the mean flow (Bretherton 1969; Durran 1995) or resulting in downslope windstorms which scour the boundary layer from the surface (Clark and Peltier 1977; Peltier and Clark 1979; Peltier and Clark 1983).

This study examines these issues in the context of a series of parallel ridges separated by shallow valleys with depths comparable to that of the nocturnal inversion. The chosen location in central Pennsylvania features from northwest to southeast: the Allegheny Plateau, the relatively narrow Bald Eagle Valley, the low Bald Eagle Ridge, a broader basin and finally the larger Tussey Ridge (Figure 1). Thus, two wave systems will be discussed, that in the lee of the Allegheny Front and that in the lee of Bald Eagle Ridge. Likewise, two drainage flow and cold pool systems are involved. The highest resolution grid of the model domain actually includes other valleys on either side of this region, but the current study focuses on this limited area and the complex interaction of lee waves and drainage flow that occurred during one nocturnal simulation.

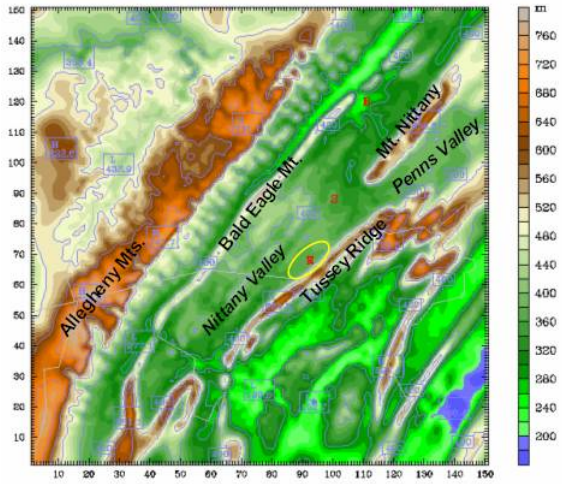

Figure 1. Topography of WRF on Domain 5, horizontal grid spacing 444 m.

2. NUMERICAL MODEL AND EXPERIMENT DESIGN

The model chosen for this research is the Weather Research and Forecasting (WRF) system's Advanced Research WRF (ARW) version 2.2 (Skamarock et al. 2005). To study the evolution of stable flows in central Pennsylvania, WRF-ARW was configured with five nested domains, each having a one-way interface with the next smaller grid. Table 1 gives the grid resolutions, time steps and number of horizontal points in each domain, while Figure 2 shows domain locations. The finest domain is centered over the Nittany Valley of central Pennsylvania and covers ~67 km X 67 km with a horizontal grid spacing of 444 m; its horizontal extent was shown in Figure 1.

Domain No.	Horiz. Res. (km)	Time Step (s)	No. of Points
1	36.000	60	141 x 91
2	12.000	45	130 x 127
3	4.000	15	193 x 169
4	1.333	5	121 x 121
5	0.444	2	151 x 151

Table 1. Resolution, time step and size of nested-grid WRF domains. All domains have 41 layers in vertical.

* *Corresponding author address*: George S. Young, 503 Walker Building, Department of Meteorology, The Pennsylvania State University, University Park, PA 16802; e-mail: Young@meteo.psu.edu

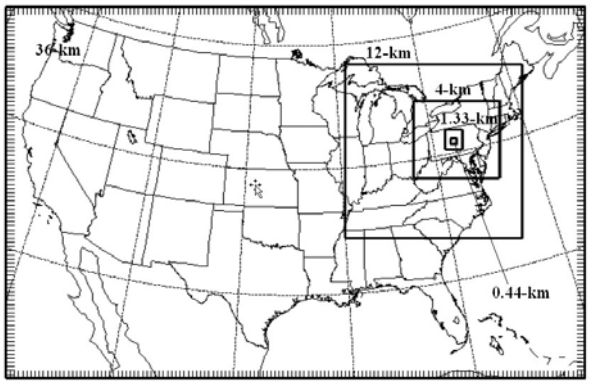

Figure 2. Five-domain nested grid configuration of WRF.

The model experiments possess 41 layers, with 10 layers in the lowest 50 m above ground level (AGL) (Figure 3a). The lowest 5 layers in this high-resolution configuration have thicknesses of 2 m each, after which the layer depths gradually increase with height up to the model top at 50 hPa. This vertical resolution near the surface is much finer than what is normally used within mesoscale model forecasts (e.g., Figure 3b), and is designed to resolve the structure of the stable boundary layer (SBL) and its dominant physical processes. The sub-kilometer WRF forecasts were run daily for 12 h during the nocturnal period, beginning at 0000 UTC, throughout the fall 2007 season. Since in nocturnal stable conditions the scale of the largest eddies is considerably less than even the horizontal grid spacing of the finest grid, the use of a Reynolds-averaged Navier-Stokes turbulence parameterization is appropriate. All experiments were run with the Mellor-Yamada-Janjic (MYJ) turbulence scheme (Janjic 2002), the Dudhia shortwave / RRTM longwave radiation schemes, simple ice microphysics, and the thermal diffusion five-layer soil model (Skamarock et al. 2005). Output files on the entire 1.333- and 0.444-km domains were saved at 12-minute intervals.

3. METEOROLOGICAL SITUATION

The case study selected for analysis was October 7, 2007, with the model run extending from 0000 to 1200 UTC. During this nocturnal period NCEP surface analyses show benign weather with weak surface wind in central Pennsylvania as a result of an anticyclone centered in Virginia. A cold front slowly approaching from the north did not reach the study domain (Figure 1) until after the end of the simulation. GOES-East IR imagery reveals cloudiness entering the area late in the night in association with this front. Thus, the weather during all but the pre-dawn hours of the night was suitable for radiative cooling and the consequent formation of drainage flows on the slopes and cold air pooling in the valleys.

This synoptic setting is reflected in the WRF simulation with light winds at ridge-top height generally from the northwest, roughly perpendicular to the terrain. Valley floor winds were light and variable, responding to both drainage flows and mountain lee waves as will be discussed in the next section.

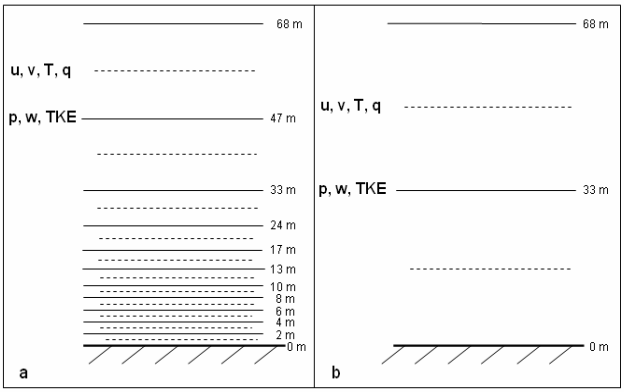

Figure 3. WRF vertical configurations below 68 m AGL. High vertical-resolution configuration shown in (a); conventional vertical-resolution configuration shown in (b).

4. MODEL RESULTS AND INTERPRETATION

4.1 *Nocturnal Cold Pool and Lee Wave Formation*

The evolution of boundary layer temperature during the early portions of the evening was as expected for such a benign synoptic setting with cooling extending up to at least several hundred meters above the surface leading to the formation of a nocturnal inversion with a depth of at least twice the mountain height (Figure 4).

As the nocturnal stable layer deepened past the top of the highest terrain mountain lee waves began to form. The terrain-perpendicular cross sections in Figure 4 show a single wave crest in the lee of the Allegheny Plateau (j ~ 5) and another in the lee of Bald Eagle Ridge (j ~ 10). Underlying each wave crest is a local maximum of turbulence kinetic energy (TKE). There are also local maxima in the surface layer of the flow descending the Allegheny Plateau and in the flow over Bald Eagle Ridge. While the latter probably result from shear production in the surface layer the former are probably associated with rotor circulations as described in previous studies (e.g. Grubišić 2008; Doyle and Durran 2002).

At this early stage in their development, both wave crests are nearly vertical in the virtual potential temperature field although they tilt downwind (i.e. to the right) with height in the in-plane wind speed field. This tilt may result from an increase in mean in-plane wind speed with height. Although not yet significantly affecting the wave structure and behavior it is worth noting that the zero contour of in-plane wind speed lies at a height near the crest of Bald Eagle Ridge with the valley floors predominantly exhibiting reverse flow (i.e. right-to-left).

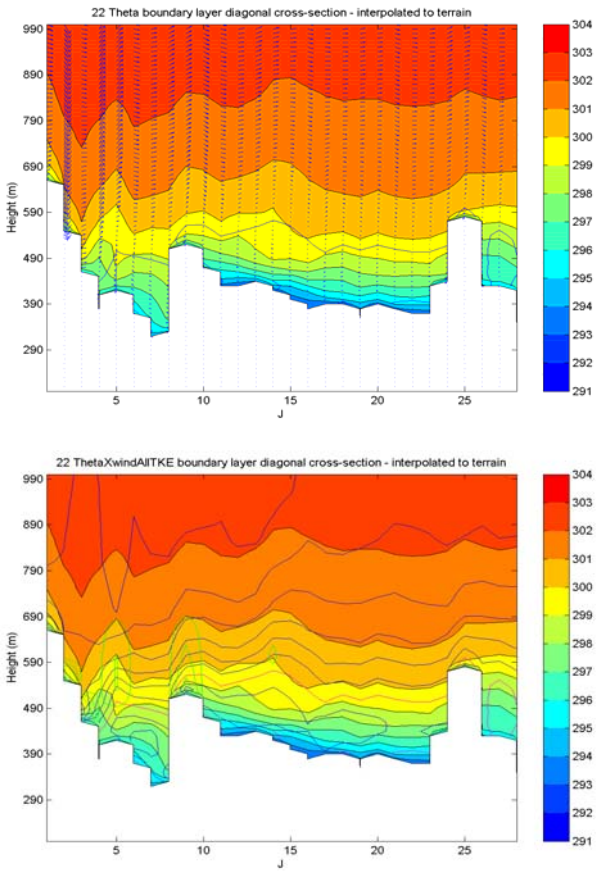

Figure 4. Terrain-perpendicular cross-section of potential temperature with an overlay of in-plane wind vectors (top) and in-plane wind speed (blue contours, bottom) and TKE (green contours, bottom) for 0424 UTC. The zero contour of in-plane wind speed is highlighted in blue (top) and pink (bottom). These cross-sections extend diagonally northwest to southeast across the central third of Figure 1 (j from 66 to 93 and i from 55 to 102 in that map's coordinate system).

4.2 *Wave Breaking and Downwind Propagation*

The effects of this flow reversal become more pronounced as the night progresses. By 0636 UTC (Figure 5) the wave crest downwind of Bald Eagle Ridge is tilting downshear (i.e. to the right with height) as much in the potential temperature field as it is in the in-plane wind speed, although the in-plane wind speed crest continues to lie about ¼ wavelength downshear of that in potential temperature. The rotor TKE maximum remains associated with the crest in the potential temperature wave, thus lying in the high-shear zone upwind of the in-plane wind speed wave crest.

As a harbinger of things to come the potential temperature contours near the level of zero in-plane wind speed (i.e. at the flow reversal level) have tilted into the vertical downwind of the potential temperature wave crest. Thus, the flow reversal is causing the wave to break downshear as observed in previous studies (e.g. Doyle et al. 2000). In those studies, however, flow weakened aloft, so the wave broke toward the mountain with the breaking at or near the upper reaches of the wave. In contrast, in the current case the wind strengthens with height. Rather than being in the upper reaches of the wave the critical level is located at approximately the same elevation as the ridge-top. Thus, it is the bottom rather than the top of the wave which breaks in this case; moreover it breaks away from the mountain rather than towards it.

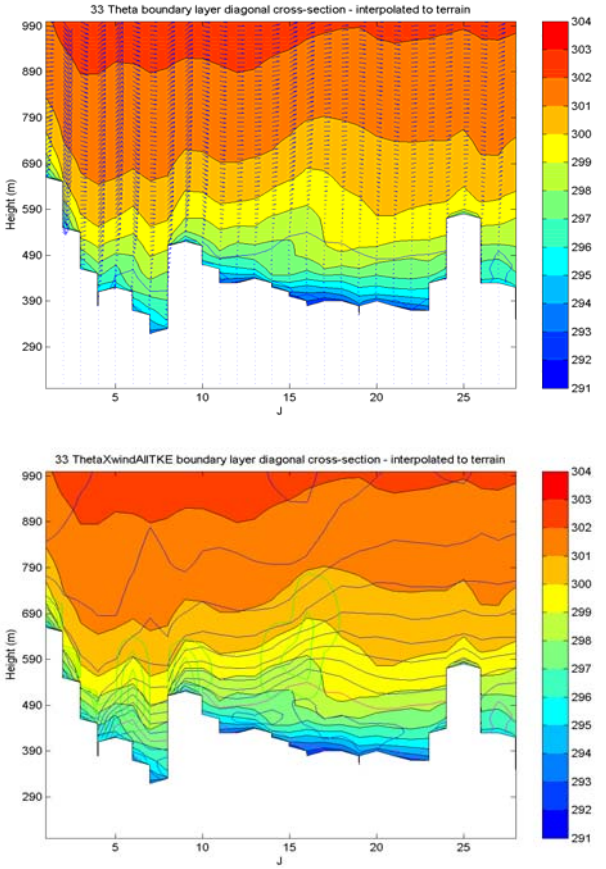

Figure 5. Same as figure 4, but for 0636 UTC.

This fundamental difference leads to behavior rather different from the downslope windstorms associated with traditional "toward mountain" wave breaking (Clark and Peltier 1977; Peltier and Clark 1979; Peltier and Clark 1983). By 0800 UTC the breaking wave has severed its connection to Bald Eagle Ridge and is propagating downwind across the intervening basin towards Tussey Ridge (Figure 6). Wave structure has also changed during this transition from standing to propagating modes. The wave crests in potential temperature and in-plane wind speed are now more closely in phase, although both continue to tilt down shear, most steeply near the level of wave breaking. Moreover, TKE follows the shifting shear zone, so that the local maximum lies not under the

potential temperature wave crest (as it does in the rotor of a standing mountain lee wave), but rather is located in the high-shear zone upwind of the crest. Thus, as the wave changed modes from standing to propagating the forcing for the TKE appears to have changed from buoyant production to shear production.

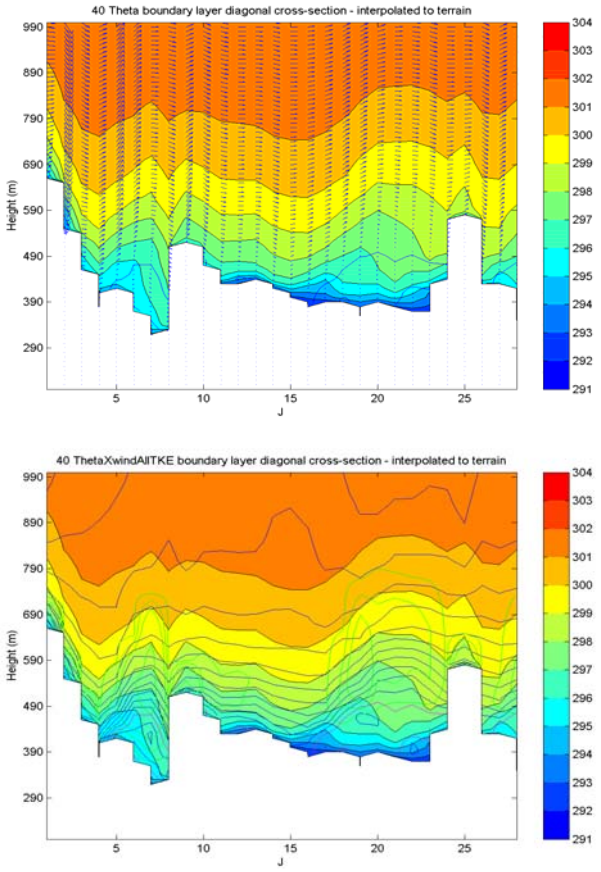

Figure 6. Same as figure 4, but for 0800 UTC.

One result of this change is that the turbulence is now positioned to mix momentum and heat down towards the surface. Thus, the northwesterly (i.e. left-to-right) flow penetrates to the surface across the upwind (i.e. left) half of the basin. The turbulence likewise erodes the cold pool from above, warming the lower levels in the upwind half of the basin. The wave's trailing edge thus has some of the key features of a turbulent wind bursts commonly observed in nocturnal inversions over flat terrain (Prabha et al. 2007).

The wave's downwind propagation results in its crest impacting Tussey Ridge by 0936 UTC (Figure 7). The potential temperature and in-plane wind speed contours remain closely aligned in the wave crest with TKE still concentrated in the high-shear zone upwind of the crest. The cold pool scouring has proceeded downwind as well, with a sharp boundary forming near the surface between the relatively warm scouring flow and the remnants of the original nocturnal cold pool with its weak reverse flow. The remnants of the cold pool are thus dammed against the slopes of Tussey Ridge (j ~ 25) disrupting to some extent the free downwind propagation of the wave. The wave did, however, reform in the next basin downwind and continue towards the southeast for the remainder of the simulation (not shown).

In a possibly unrelated event the wave in the lee of the Allegheny plateau amplifies by 0936 UTC (Figure 7) and overwhelms the flow over Bald Eagle Ridge leading to a wave tough over that feature and a second wave crest in its immediate lee.

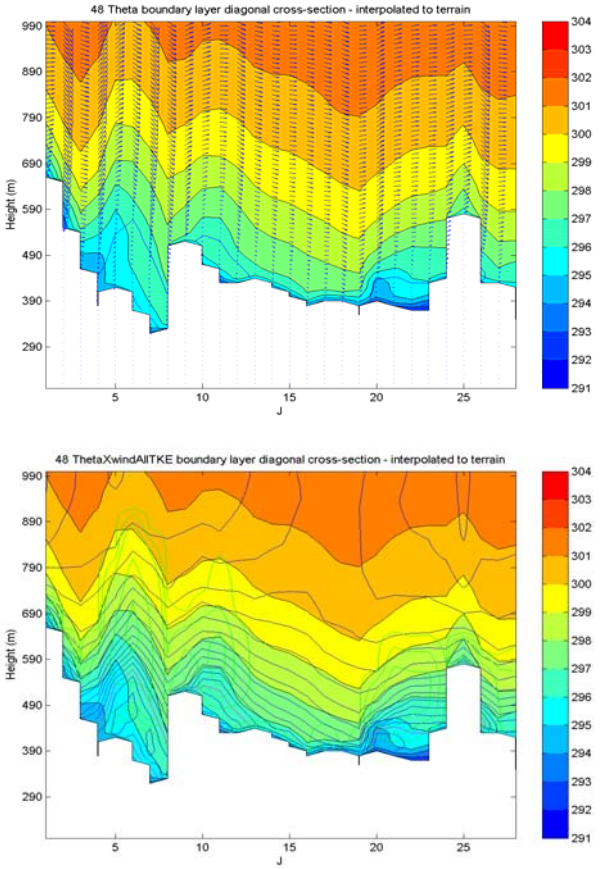

Figure 7. Same as figure 4, but for 0936 UTC.

These processes continue through the rest of the night. By 1100 UTC (Figure 8), the wave has pushed off the right side of the cross-section while the remnants of the cold pool and reverse flow have been almost completely scoured from the upwind base of Tussey Ridge. Simultaneously the lee wave from the Allegheny Plateau continues to extend downwind, now with three crests, two of them in the lee of Bald Eagle Ridge. Unencumbered by reverse flow these waves retain the vertical phase planes associated with horizontally propagating mountain lee waves (Scorer 1949; Durran 1995).

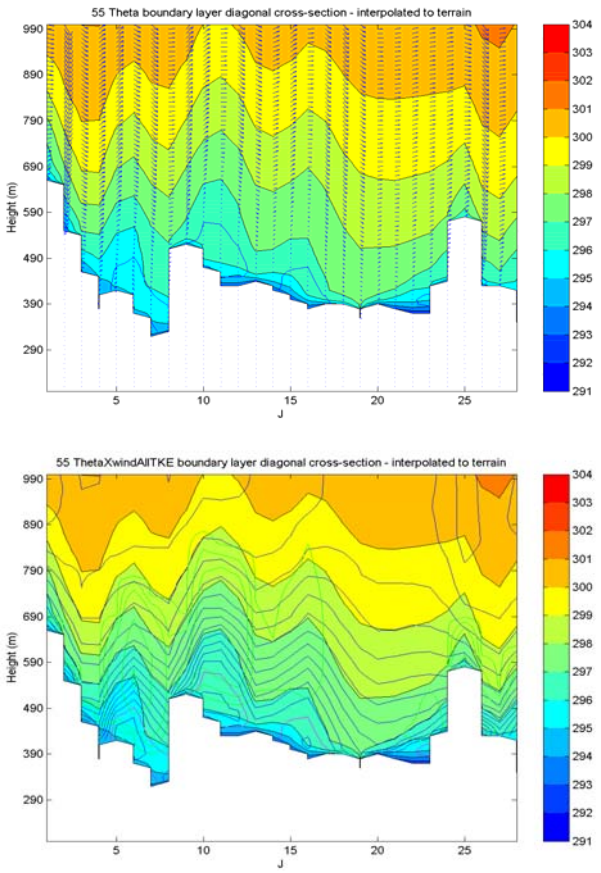

Figure 8. Same as figure 4, but for 1100 UTC.

5. SUMMARY

In this study, a specially configured version of WRF-ARW has been used to investigate the interaction of mountain lee waves in the nocturnal inversion with a low-level (i.e. below ridge crest) flow reversal. While the growth of the nocturnal inversion provided a stability environment suitable for growth of standing mountain lee waves, the existence of low-level reverse flow in one basin caused the wave therein to tilt away from the generating mountain and eventually to break near the level of the flow reversal. Subsequent to the wave's breaking it propagated downwind and changed structure such that the TKE maximum moved from the rotor position under the crest into the tilted high-shear zone upwind of the crest. The wave then began propagating downwind trailed by an intensifying momentum and temperature mix-down event. The latter eventually scoured the nocturnal cold pool from the basin. This sequence of events took most of the night to complete and resulted in a significant alteration of the diurnal cycle of valley-floor winds and temperatures from that which would occur on a night with no mesoscale disturbances.

Acknowledgements: This research has been sponsored by the Defense Threat Reduction Agency under contract no. W911NF-06-1-0439-MOD-P00001 under the supervision of Dr. John Hannan. We also acknowledge Mr. Glenn Hunter and Ms. Karen Tinklepaugh of Penn State for assistance with data access as well as Mr. Lorne Leonard and Mr. Joshua Gelman for valuable suggestions concerning analysis displays.

6. REFERENCES

Beal, R.C., G.S. Young, F.M. Monaldo, D.R. Thompson, S. Carven, 2005: High Resolution Wind Monitoring with Wide Swath SAR: A Users Guide. National Oceanic and Atmospheric Administration; National Environmental Satellite, Data, and Information Service; Office of Research and Applications, Washington D.C. 155pp.

Bretherton, F. P., 1969: Momentum transport by gravity waves. *Quart. J. Roy. Meteor. Soc.,* **95,** 213–243.

Clark, T. L., and W. R. Peltier, 1977: On the evolution and stability of finite amplitude mountain waves. *J. Atmos. Sci.,* **34,** 1715–1730.

Doyle, J.D., and D.R. Durran, 2002: The Dynamics of Mountain-Wave-Induced Rotors. *J. Atmos. Sci.*, **59**, 186–201.

Doyle, J.D., D.R. Durran, C. Chen, B.A. Colle, M. Georgelin, V. Grubisic, W.R. Hsu, C.Y. Huang, D. Landau, Y.L. Lin, G.S. Poulos, W.Y. Sun, D.B. Weber, M.G. Wurtele, and M. Xue, 2000: An Intercomparison of Model-Predicted Wave Breaking for the 11 January 1972 Boulder Windstorm. *Mon. Wea. Rev.*, **128**, 901–914.

Durran, D.R., and J.B. Klemp, 1983: A Compressible Model for the Simulation of Moist Mountain Waves. *Mon. Wea. Rev.*, **111**, 2341–2361.

Durran, D.R., 1995: Do Breaking Mountain Waves Decelerate the Local Mean Flow? *J. Atmos. Sci.*, **52**, 4010–4032.

Fast, J.D., S. Zhong, and C.D. Whiteman, 1996: Boundary Layer Evolution within a Canyonland Basin. Part II: Numerical Simulations of Nocturnal Flows and Heat Budgets. *J. Appl. Meteor.*, **35**, 2162–2178.

Galperin, B., S. Sukoriansky, and P.S. Anderson, 2007: On the critical Richardson number in stably stratified turbulence. *Atmos. Sci. Let.*, **8**, 65-67.

Grubišić, V., J.D. Doyle, J. Kuettner, S. Mobbs, R.B. Smith, C.D. Whiteman, R. Dirks, S. Czyzyk, S.A. Cohn, S. Vosper, M. Weissmann, S. Haimov, S.F.J. De Wekker, L.L. Pan, and F.K. Chow, 2008: The Terrain-Induced Rotor Experiment. *Bull. Amer. Meteor. Soc.*, **89**, 1513–1533.

Janjic, Z.I., 2002: Nonsingular implementation of the Mellor-Yamada Level 2.5 Scheme in the NCEP Meso model. NCEP Office Note 437, 61 pp.

Jiang Q., and J. D. Doyle, 2008: Diurnal variation of downslope winds in Owens Valley during the Sierra Rotor Experiment. *Mon. Wea. Rev.*, **136**, 3760–3780.

Peltier, W. R., and T. L. Clark, 1979: The evolution and stability of finite-amplitude mountain waves. Part II: Surface wave drag and severe downslope windstorms. *J. Atmos. Sci.,* **36,** 1498–1529.

——, and ——, 1983: Nonlinear mountain waves in two and three spatial dimensions. *Quart. J. Roy. Meteor. Soc.,* **109,** 527–548.

Prabha, T.V., M.Y. Leclerc, A. Karipot, and D.Y. Hollinger, 2007: Low-Frequency Effects on Eddy Covariance Fluxes under the Influence of a Low-Level Jet. *J. Appl. Meteor. Climatol.*, **46**, 338–352.

Skamarock, W.C., J.B. Klemp, J. Dudhia, D.O. Gill, D.M. Barker, W. Wang, and J.G. Powers, 2005: A description of the advanced research WRF version 2. NCAR Tech. Note NCAR/TN-468+STR, 88 pp.

Scorer, R., 1949: Theory of Waves in the Lee of mountains. *Quart. J. Roy. Meteor. Soc*., **75**, 41-56.

Zhong, S., C.D. Whiteman, X. Bian, W.J. Shaw, and J.M. Hubbe, 2001: Meteorological Processes Affecting the Evolution of a Wintertime Cold Air Pool in the Columbia Basin. *Mon. Wea. Rev*., **129**, 2600–2613.